Myocardial Emission Computed Tomography with Iodine-123-Labeled Beta-Methyl-Branched Fatty Acid in Patients with Hypertrophic Cardiomyopathy

Chinori Kurata, Kei Tawarahara, Takahisa Taguchi, Shigeyuki Aoshima, Akira Kobayashi, Noboru Yamazaki, Hiroaki Kawai, and Masao Kaneko

Third Department of Internal Medicine and Department of Radiology, Hamamatsu University School of Medicine, Hamamatsu, Japan

We studied whether emission computed tomography (ECT) with ^{123}I-labeled 15-(p-iodophenyl)-3R,S-methylpentadecanoic acid (BMIPP) shows myocardial distribution different from ^{201}Tl in hypertrophic cardiomyopathy. In 10 patients with asymmetric septal hypertrophy (ASH), 5 with diffuse hypertrophy and 2 with apical hypertrophy, ECT was acquired 30 min (early) and 4 hr (late) after injection of ^{123}I-BMIPP at rest and was compared with ECT with ^{201}Tl. In 10 patients with ASH, the relative regional uptake (RRU) of the septum was lower in the early ^{123}I-BMIPP study than in the ^{201}Tl study, although that of the posterior wall was similar. In the early and late ^{123}I-BMIPP studies, the RRU of the septum was lower in 10 patients with ASH than in 7 without ASH, although that of the posterior wall was similar. In the ^{201}Tl study, however, the RRU of both the septum and posterior wall was similar in those with and without ASH. Moreover, in 16 patients, the apparent left ventricular size was larger in the early ^{123}I-BMIPP study than in the ^{201}Tl study, which suggested reduced ^{123}I-BMIPP uptake in the subendocardium. In patients with hypertrophic cardiomyopathy, thus, ^{123}I-BMIPP imaging may reveal impaired regional fatty acid utilization, which is independent of regional perfusion.

J Nucl Med 1992; 33:6–13

Myocardial metabolic imaging has been expected not only to enhance our understanding of cardiomyopathies, but also to aid in the development of effective treatment of cardiomyopathies (*1*). Recently, several studies using PET have demonstrated regional changes in myocardial metabolism in patients with cardiomyopathy (*2–6*). Unfortunately, positron imaging is not widely available at present. Several radioiodinated fatty acids have been used for investigating myocardial accumulation and turnover of fatty acids in patients with dilated cardiomyopathy, ischemic heart disease and hypertensive hypertrophy (*7–12*). It, however, remains unclear whether metabolic imaging with radioiodinated fatty acids can elucidate the characteristic features of patients with hypertrophic cardiomyopathy (HCM).

Myocardial perfusion imaging with ^{201}Tl has demonstrated regional perfusion abnormalities in patients with various cardiomyopathies (*13–18*). Perfusion defects in those patients might represent myocardial scar and/or ischemia. If an uncoupling of regional perfusion and fatty acid utilization exists in the myocardium of cardiomyopathy, myocardial imaging with radioiodinated fatty acids could elucidate unique features different from ^{201}Tl imaging. In the cardiomyopathic Bio 14.6 Syrian hamster, an animal model for HCM, we have demonstrated discrepancies in the myocardial distributions of ^{201}Tl and ^{125}I-labeled 15-(p-iodophenyl)3R,S-methylpentadecanoic acid (BMIPP) (*19*). The present study was therefore undertaken to investigate whether emission computed tomography (ECT) with ^{123}I-BMIPP may show myocardial distribution different from that with ^{201}Tl in patients with HCM.

METHODS

Patients Characteristics

The study group consisted of 17 patients (11 men and 6 women), ranging in age from 21 to 75 yr (Table 1). In all 17 patients, left ventricular hypertrophy was diagnosed on echocardiographic demonstration. Two of these 17 patients had coronary artery disease; one had a significant stenosis of the right coronary artery, hypertension and diabetes mellitus; and the other patient had three-vessel disease with previous myocardial infarction. The two patients, however, were diagnosed as having HCM as a complication because their hypertrophy, limited to the interventricular septum, could not be explained by coronary artery disease alone. The remaining 15 of these 17 patients had normal coronary angiograms and were diagnosed as having HCM because their left ventricular hypertrophy could not be ascribed to another cardiac or systemic disease.

Received Mar. 28, 1991; revision accepted Jul. 11, 1991.

For reprints contact: Chinori Kurata, MD, The Third Department of Internal Medicine, Hamamatsu University School of Medicine, 3600 Handa-cho, Hamamatsu, 431-31 Japan.

TABLE 1
Clinical and Echocardiographic Features of Patients

Patient	Age	Sex	Type of HCM	IVSth	LVPWth	LVDd	LVDs	LVEF
1	71	M	ASH	20	12	45	25	83
2	42	M	ASH	22	10	43	31	63
3	58	M	ASH	20	13	48	28	80
4	66	M	ASH	20	13	49	38	53
5	49	F	ASH	22	10	45	30	70
6	50	F	ASH	25	12	43	27	75
7	54	M	ASH	18	10	42	36	37
8	21	F	ASH	15	8	33	17	86
9	75	F	ASH	26	10	45	23	87
10	75	F	ASH	16	9	32	26	46
11	65	F	Diffuse	21	19	35	20	81
12	70	M	Diffuse	30	30	32	30	76
13	57	M	Diffuse	26	22	56	31	83
14	53	M	Diffuse	30	26	32	12	95
15	56	M	Diffuse	27	25	35	15	92
16	68	M	Apical	12	10	52	30	81
17	56	M	Apical	14	10	46	28	77

HCM = hypertrophic cardiomyopathy; IVSth = end-diastolic thickness of the septum (mm); LVPWth = end-diastolic thickness of the posterior wall (mm); LVDd = end-diastolic left ventricular dimension (mm); LVDs = end-systolic left ventricular dimension (mm); LVEF = left ventricular ejection fraction (%); and ASH = asymmetric septal hypertrophy.

Echocardiographic Studies

Echocardiographic studies were performed within a week of ^{123}I-BMIPP imaging, using a phased-array scanner operating at 2.5 or 3.5 MHz (Model SSD870, Aloka, Tokyo, Japan). The M-mode echocardiographic examination was performed by moving an M-mode cursor on the two-dimensional parasternal long-axis view. The M-mode echocardiographic measurements were performed according to the criteria recommended by the American Society of Echocardiography (*20*) and the results are shown in Table 1.

Asymmetric septal hypertrophy (ASH) was considered to be present if the end-diastolic thickness of the septum was at least 15 mm and its ratio to that of the left ventricular posterior wall was at least 1.3. Diffuse hypertrophy was considered to be present if both of the end-diastolic thicknesses of the septum and posterior wall were at least 15 mm. If echocardiographic apical long-axis or four-chamber view demonstrated apical hypertrophy and a characteristic spade-like configuration was demonstrated in the right anterior oblique ventriculogram at end-diastole (*21*), apical hypertrophy was considered to be present. According to these criteria, 10 had ASH, 5 had diffuse hypertrophy and 2 had apical hypertrophy (Table 1). The two patients with coronary artery disease (Patients 9 and 10) had ASH.

ECT Acquisitions

All patients gave informed consent to a protocol of ^{123}I-BMIPP imaging as a Phase 2 clinical trial. The study protocol and consent form had been approved by the Hamamatsu University School of Medicine Human Subject Protection Committee. On the day of ^{123}I-BMIPP imaging, patients had no breakfast and continued fasting until the end of the late imaging session. At rest, 111 MBq (3 mCi) of ^{123}I-BMIPP were injected intravenously. Early tomographic imaging was started 30 min after the injection, using a large field of view rotating gamma camera equipped with a low-energy, all-purpose collimator centered on the 159 keV photo peak with a 20% window. The camera was rotated over 180 degrees from the 45-degree right anterior oblique to the 45-degree left posterior oblique position. Thirty-two images were obtained in a 64 × 64 matrix for 30 sec per image on a dedicated nuclear medicine computer (Scintipac 2400, Shimadzu, Kyoto, Japan). No attenuation or scatter correction was used. Late imaging was performed 4 hr after injection using the same imaging protocol as that for early imaging.

Four or six days after the ^{123}I-BMIPP studies, ^{201}Tl imaging was performed after an overnight fast. At rest, 111 MBq (3 mCi) of ^{201}Tl were injected intravenously. Emission computed tomograms were acquired 10 min after injection using the same imaging protocol as that for ECT with ^{123}I-BMIPP except that the energy discrimination centered at 70 keV with a 20% window.

For each of the ^{201}Tl and early and late ^{123}I-BMIPP acquisition data, the same reconstruction of tomographic images were performed. Each data set was reconstructed by a Shepp-Logan filtered backprojection algorithm after preprocessing of the projection images with Butterworth filter correction as 1-pixel thick transverse slices. Vertical long-axis, short-axis and horizontal long-axis slices, each 6 mm thick, were reconstructed from the transverse slices and were magnified two diameters using the same left ventricular oblique angles for each of the ^{201}Tl and early and late ^{123}I-BMIPP data.

Quantitative Analysis of Tomograms

From each set of the ^{201}Tl and early and late ^{123}I-BMIPP short-axis slices, three composite slices 18 mm or 24 mm thick were constructed by adding three or four short-axis slices, respectively. The same number of short-axis slices (three or four) was used to reconstruct the composite slices for each of the ^{201}Tl and early and late ^{123}I-BMIPP studies in each patient. The three composite slices consisted of basal, mid- and apical ventricular levels. The composite basal and mid-ventricular slices were divided, respectively, into eight segments, and the composite apical ventricular slice was divided into five segments (Fig. 1). A square region of interest of 5 × 5 pixels was placed over the center of each of the

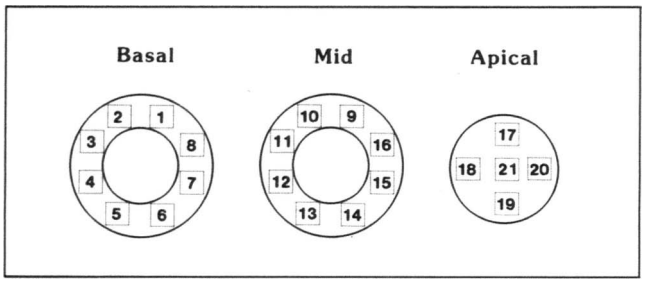

FIGURE 1. Three reconstructed short-axis slices: basal, mid and apical slices. Eight square regions of interest of 5 × 5 pixels were placed on the basal and mid slices, and five square regions of interest of 5 × 5 pixels were placed on the apical slice. The anterior region consists of Segments 1, 2, 9, 10, and 17. The septal region consists of Segments 3, 4, 11, 12, and 18. The inferior region consists of Segments 5, 6, 13, 14, and 19. The lateral region consists of Segments 7, 8, 15, 16, and 20.

total 21 segments. For each segment, the regional uptake was determined for each segment as mean counts per pixel within the corresponding region of interest. Moreover, the relative regional uptake (RRU, %) was determined for each segment as the ratio of its regional uptake to the maximum regional uptake within the total 21 segments of each set of the three composite short-axis slices. In the ^{123}I-BMIPP studies, the washout rate (%) in each segment was calculated by subtracting regional uptake in the late image from the corresponding regional uptake in the early image and dividing by that in the early image.

Apparent Left Ventricular Size

In our previous experimental study using cardiomyopathic hamsters, more ^{123}I-BMIPP accumulated in the epicardial side of the left ventricular myocardium than in the endocardial side, although ^{201}Tl accumulated almost equally in the epicardial and endocardial sides (*19*). If the experimental findings could be applied to human cardiomyopathy, the apparent size of the left ventricular cavity on the ^{123}I-BMIPP tomogram might be larger than that on the ^{201}Tl tomogram. The apparent left ventricular size was therefore compared between the ^{201}Tl and early ^{123}I-BMIPP tomograms, using the following method. A short-axis slice in the mid- to basal ventricular level from each of the ^{201}Tl and early ^{123}I-BMIPP studies was chosen so that two short-axis slices from the two studies anatomically corresponded to each other. In the short-axis slice, the center was assigned from which 60 equidistant radii (6 degrees apart) were generated toward the left ventricular periphery. A region of interest was generated by connecting 60 points with the maximum counts per pixel within each radius. The apparent left ventricular size was evaluated with the number of pixels within the region of interest.

Statistical Methods

The data are presented as mean ± s.d. The statistical significance of differences in mean values between two groups was analyzed with the paired or unpaired Student's t-test. When test groups were not normally distributed, the paired or unpaired nonparametric Wilcoxon t-test was applied. Correlations between two variables were examined using linear regression analysis. Probability (p) values of <0.05 (two-sided) were considered to be statistically significant.

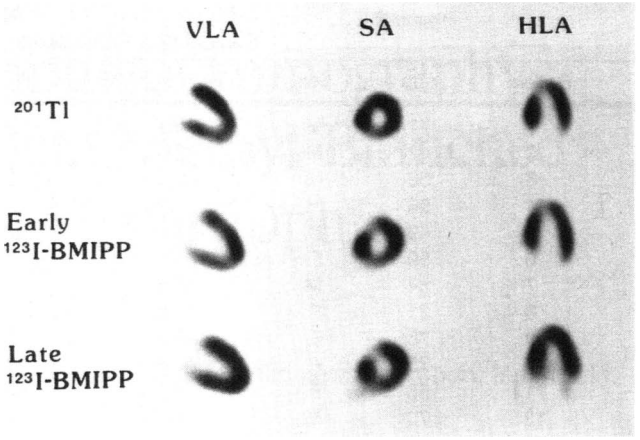

FIGURE 2. Vertical long-axis (VLA), short-axis (SA) and horizontal long-axis (HLA) slices in the ^{201}Tl and early and late ^{123}I-BMIPP studies from Patient 11 with diffuse hypertrophy. The quality of the myocardial tomograms with ^{123}I-BMIPP is as good as those with ^{201}Tl.

RESULTS

Regional Uptakes of ^{201}Tl and ^{123}I-BMIPP

In all of the early and late studies, ^{123}I-BMIPP provided high contrast tomograms of the left ventricular myocardium (Fig. 2), although the quality of the late ^{123}I-BMIPP images was relatively poor compared with the ^{201}Tl and early ^{123}I-BMIPP images.

The mean regional uptake of the total 357 segments (17 patients × 21 segments/patient) was 445 ± 216, 228 ± 81 and 133 ± 38 counts/pixel in the ^{201}Tl and early and late ^{123}I-BMIPP studies, respectively. The regional uptakes of ^{201}Tl correlated with those of ^{123}I-BMIPP in the early study ($r = 0.781$; $p < 0.001$) and in the late study ($r = 0.664$; $p < 0.001$). The regional uptakes of ^{123}I-BMIPP in the late study correlated with those in the early study ($r = 0.904$; $p < 0.001$). Regional uptake was significantly higher in the ^{201}Tl study than in the early ^{123}I-BMIPP study ($p < 0.001$). In the 357 segments, the washout rate of ^{123}I-BMIPP from the early to the late study was 40.1% ± 9.4%.

Relative Regional Uptake of ^{201}Tl and ^{123}I-BMIPP

In the 357 segments, the RRU was 75.5% ± 15.4%, 75.8% ± 15.2% and 77.5% ± 14.3% in the ^{201}Tl and early and late ^{123}I-BMIPP studies, respectively. The RRU of ^{201}Tl correlated with those of ^{123}I-BMIPP in the early study ($r = 0.714$; $p < 0.001$) and in the late study ($r = 0.618$; $p < 0.001$). The RRU of ^{123}I-BMIPP in the late study correlated with that in the early study ($r = 0.863$; $p < 0.001$).

The mean difference in the RRU between the ^{201}Tl and early ^{123}I-BMIPP studies was 0.3% ± 11.6% (RRU of ^{123}I-BMIPP minus RRU of ^{201}Tl). The distribution of the differences in the 357 segments is shown in Figure 3A. The absolute value of the difference in the RRU between the ^{201}Tl and early ^{123}I-BMIPP studies was greater than 10% in 146 (41%) of the 357 segments and than 20% in 29 segments (8%). Similarly, the mean difference in the

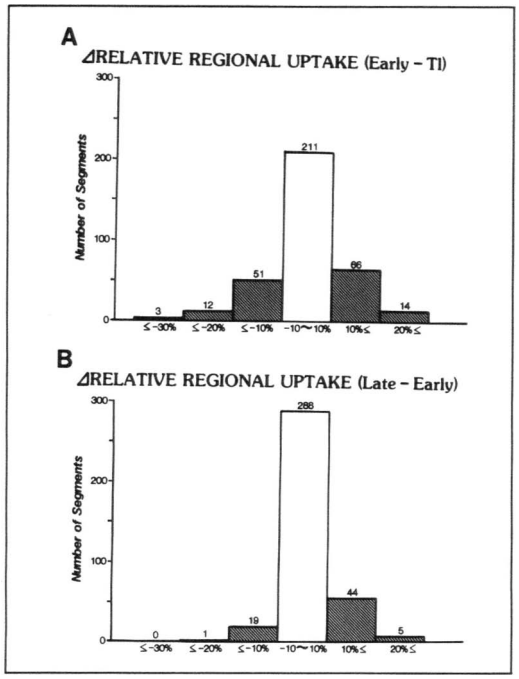

FIGURE 3. (A) Distribution of the difference in relative regional uptake (RRU) between the ^{201}Tl and early ^{123}I-BMIPP studies in 357 segments. The RRU of ^{123}I-BMIPP in a segment minus that of ^{201}Tl in the corresponding segment (Δ Relative Regional Uptake (Early–Tl)) on the x-axis is classified into six levels: ≦−30% (−40<, ≦−30%), ≦−20% (−30%<, ≦−20%), ≦−10% (−20%<, ≦−10%), −10% ~ 10% (−10%<, <10%), 10%≦ (10%≦, <20%), and 20%≦ (20%≦, <30%). Hatched bars represent segments with the absolute value of the Δ relative regional uptake greater than 10%. (B) Distribution of the difference in RRU between the early and late ^{123}I-BMIPP studies. The RRU in the late study minus that in the early study (Δ Relative Regional Uptake (Late–Early)) is classified in the same manner as in A above.

RRU between the early and late ^{123}I-BMIPP studies was 1.8% ± 7.7% (RRU in the late study minus RRU in the early study). The distribution of the differences in the 357 segments is shown in Figure 3B. The absolute value of the difference in the RRU between the early and late ^{123}I-BMIPP studies was greater than 10% in 69 (19%) of the 357 segments and than 20% in 6 segments (1.7%).

Apparent Size of the Left Ventricle

The left ventricular cavity was apparently larger in the ^{123}I-BMIPP study than in the ^{201}Tl study, particularly in patients with diffuse hypertrophy (Fig. 4). The ratio of the apparent left ventricular size in the early ^{123}I-BMIPP study to that in the ^{201}Tl study was 1.20 ± 0.03 in 17 patients. The ratio in the 16 patients was greater than 1.0. To examine whether the finding might be due to an artifact of reconstruction or attenuation, we performed an experiment using a left ventricular myocardium phantom and the same imaging protocol as in the clinical study. As a result, the ratio of apparent ventricular sizes in the ^{123}I-BMIPP study to that in the ^{201}Tl study was 1.03 ± 0.03, which was significantly smaller than that in the 17 patients ($p < 0.05$). Moreover, in 14 patients (82%), the ratio was greater than 1.09 (mean ± 2 s.d. in the phantom experiment).

Iodine-123-BMIPP Tomograms in Patients with ASH

In the 10 patients with ASH, the RRU of the septum (the mean of Segments 3 and 11) was 76% ± 8%, 70% ± 9% and 70% ± 11%, and the RRU of the posterior wall (the mean of Segments 6 and 14) was 75% ± 15%, 76% ± 15% and 78% ± 13% in the ^{201}Tl and early and late ^{123}I-BMIPP studies, respectively. The RRU of the septum in the early ^{123}I-BMIPP study was lower than that in the ^{201}Tl study ($p < 0.05$), although that of the posterior wall was similar in the two studies ($p > 0.05$). However, the RRU of both the septum and posterior wall was similar in the ^{201}Tl and late ^{123}I-BMIPP studies ($p > 0.05$, respectively). Figure 5 shows examples of the patients with ASH.

In the seven patients without ASH, the RRU of the septum was 79% ± 11%, 86% ± 7% and 86% ± 8%, and the RRU of the posterior wall was 76% ± 5%, 77% ± 4% and 80% ± 6% in the ^{201}Tl and early and late ^{123}I-BMIPP studies, respectively. Figure 6 shows the comparison of RRU between the 10 patients with and the 7 without ASH. In both the early and late ^{123}I-BMIPP studies, the RRU of the septum was lower in the 10 patients with ASH than in the 7 without ASH ($p < 0.01$ and $p < 0.05$, respectively), although that of the septum in the ^{201}Tl study was similar ($p > 0.05$, respectively). In all of the ^{201}Tl and early and late ^{123}I-BMIPP studies, however, the RRU of the posterior wall was similar in those with and without ASH ($p > 0.05$, respectively).

Furthermore, the ratio of the RRU in the early ^{123}I-BMIPP study to that in the ^{201}Tl study was compared between the 10 patients with and the 7 without ASH (Fig. 7). The ratio in the septum was smaller in the 10 patients with ASH (0.92 ± 0.09) than in the 7 without ASH (1.09 ± 0.10; $p < 0.01$). However, the ratio of the posterior wall

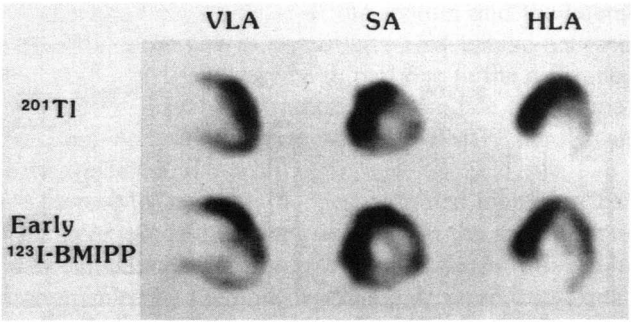

FIGURE 4. Tomograms of Patient 12 with diffuse hypertrophy. The left ventricle appears to be larger in the early ^{123}I-BMIPP images than in the ^{201}Tl images. The difference suggests that transmural distribution may not be similar in the two tracers. These tomograms also shows a matched decrease of ^{201}Tl and ^{123}I-BMIPP in the subendocardium of the inferolateral wall. However, it is not certain because the spatial resolution of this imaging is too poor to discriminate the endocardium from the epicardium. Abbreviations as in Figure 2.

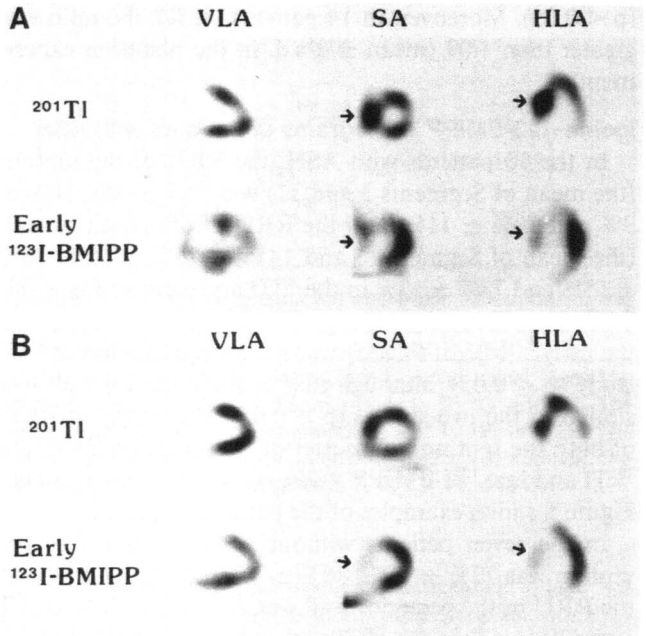

FIGURE 5. Tomograms of Patients 5A and 6B with septal hypertrophy. (A) The septal uptake (arrows) is high in the ^{201}Tl images but markedly low in the early ^{123}I-BMIPP images. (B) The uptake of ^{123}I-BMIPP (arrows) is lower in the septum than in the other regions, although that of ^{201}Tl is not so different. Abbreviations as in Figure 2.

was similar in those with and without ASH (1.03 ± 0.10 versus 1.02 ± 0.07; $p > 0.05$).

Thus, in the patients with ASH, the disproportionately thickened septum showed reduced uptake of ^{123}I-BMIPP compared to ^{201}Tl. In the two patients with ASH and congestive heart failure, however, the ^{201}Tl and ^{123}I-BMIPP tomograms demonstrated similar defects (Fig. 8).

Iodine-123-BMIPP Tomograms in Patients with Diffuse or Apical Hypertrophy

The five patients with diffuse hypertrophy showed relatively similar myocardial distributions of activity in the

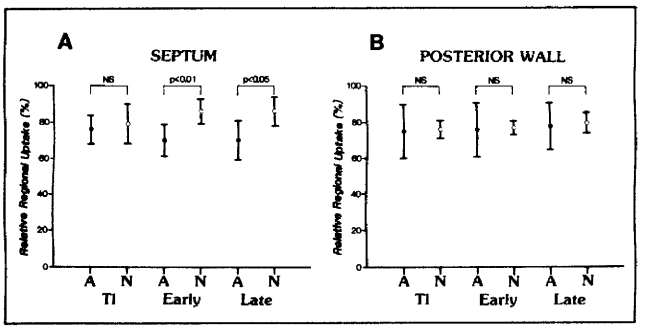

FIGURE 6. (A) Comparisons of relative regional uptakes (RRU) in the septum between the 10 patients (Group A) with and the 7 (Group N) without asymmetric septal hypertrophy. (B) Comparisons of RRU in the posterior wall between the two groups, A and N. Bars represent the mean ± s.d. of RRU in Groups A and N (NS = not significant; Tl = ^{201}Tl study; Early = early ^{123}I-BMIPP study; and Late = late ^{123}I-BMIPP study).

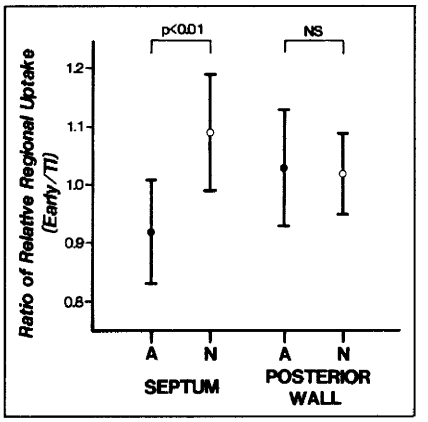

FIGURE 7. Comparisons of the ratio of the relative regional uptake in the early ^{123}I-BMIPP study (Early) to that in the ^{201}Tl study (Tl) between the 10 patients (Group A) with and the 7 (Group N) without asymmetric septal hypertrophy. (Left, comparison in the septum; Right, comparison in the posterior wall).

^{201}Tl and early and late ^{123}I-BMIPP tomograms, except for the apparent difference in left ventricular size (Figs. 2 and 4). Of the two patients with apical hypertrophy, one showed a ^{123}I-BMIPP defect in the apical region where the ^{201}Tl uptake was higher compared with the other regions (Fig. 9), although the other did not show such a discrepancy between ^{201}Tl and ^{123}I-BMIPP uptake in the apical region.

DISCUSSION

We have demonstrated that patients with HCM showed a discrepancy of myocardial distributions between ^{201}Tl and ^{123}I-BMIPP.

Iodine-123-BMIPP Tomograms in Patients with ASH

The disproportionately thickened septum in the patients with ASH showed a reduced uptake of ^{123}I-BMIPP independent of regional perfusion assessed by ^{201}Tl, although such an uncoupling of ^{201}Tl and ^{123}I-BMIPP was not detected in those without ASH. Moreover, the patients

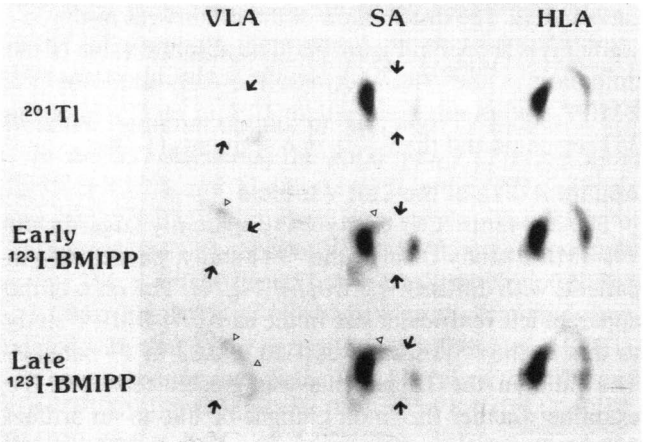

FIGURE 8. Tomograms of Patient 7 with asymmetric septal hypertrophy and heart failure. There are massive defects in the anterior and inferior regions (arrows) in the early and late ^{123}I-BMIPP studies as well as in the ^{201}Tl study. Iodine-123-BMIPP uptake in the anterior region (small open triangles) is slightly higher compared to ^{201}Tl. Abbreviations as in Figure 2.

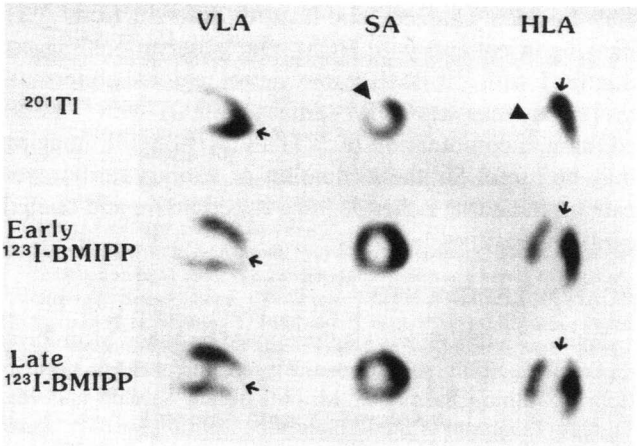

FIGURE 9. Tomograms of Patient 16 with apical hypertrophy. The apical uptake (arrows) is high in the ^{201}Tl study, but it is low in the early and late ^{123}I-BMIPP studies. Reduced ^{201}Tl uptake (large closed triangles) is noted in the anteroseptal region, but ^{123}I-BMIPP uptake is not reduced in the region. Abbreviations as in Figure 2.

with ASH and congestive heart failure, which might represent an advanced stage of HCM, showed similar defects of ^{123}I-BMIPP and ^{201}Tl. In the patients with ASH, therefore, abnormalities of myocardial fatty acid metabolism may precede impairment of perfusion or histological changes such as fibrosis.

Transmural Differences of ^{123}I-BMIPP Uptake

The apparent left ventricular size was larger in the ECT with ^{123}I-BMIPP compared to ^{201}Tl. It suggests that the hypertrophied myocardium may accumulate less ^{123}I-BMIPP in the subendocardium than in the subepicardium. Using the count peaks of profile curves on ECT with ^{201}Tl, Takeishi et al. (*22*) measured an apparent left ventricular size and compared it with left ventricular volume measured by radionuclide angiography. They concluded that dipyridamole-induced dilatation of the left ventricular cavity reflected relative subendocardial hypoperfusion. However, it has not been confirmed whether the difference in size between ECT with different isotopes such as ^{201}Tl and ^{123}I may reflect their different distributions. Comparison between ECT with ^{201}Tl and ^{123}I-BMIPP in normal controls is necessary for concluding that their transmural distributions are different than that in patients with HCM.

Comparison with Autoradiographic Studies

In previous autoradiographic studies using cardiomyopathic hamsters (*19,23*) or hypertensive rats (*24–26*), the uptake of methyl-branched fatty acids was lower in the subendocardial region than in the subepicardial region, although perfusion was similar in the two regions. In patients with HCM, similarly, the apparently larger left ventricle in the ^{123}I-BMIPP study may suggest reduced uptake of ^{123}I-BMIPP in the subendocardial region without transmural differences in perfusion.

Mechanisms of Myocardial ^{123}I-BMIPP Uptake

BMIPP was designed to have prolonged myocardial retention suitable for ECT (*27*). The insertion of a methyl radical in the beta-position inhibits beta oxidation and prolongs myocardial retention. The myocardial uptake of BMIPP, therefore, does not directly reflect beta-oxidation of fatty acids in the myocardium. In fact, recent experimental studies using carnitine acyltransferase I inhibitors, 2-tetradecylglycidic acid (*28*) or 2[5(4-chlorophenyl)-pentyl]oxirane-2-carboxylate (*29*), demonstrated that the myocardial extraction of BMIPP was not decreased by these inhibitors.

Myocardial accumulation of BMIPP has been reported to be observed mainly in the triglyceride fraction (*30*) and to be associated with the synthesis of triglyceride (*28*). Furthermore, it has been demonstrated that myocardial BMIPP accumulation may be closely correlated with intracellular concentrations of adenosine triphosphate, which is required in the first step of enzymatic conversion of fatty acids to acyl-CoA, a common pathway of fatty acid metabolism, such as triglyceride synthesis and β-oxidation (*31*). Thus, the uptake of BMIPP may reflect some aspect of myocardial fatty acid metabolism, such as incorporation into triglyceride storage products or an oxidative process responsible for the conversion of BMIPP to polar catabolites (*32*).

Mechanisms of Abnormal ^{123}I-BMIPP Distribution in HCM

Our finding indicates that the disproportionately thickened septum may have some regional impairment in fatty acid metabolism independent of perfusion. Grover-McKay et al. (*6*), using PET, reported that ^{11}C-palmitate uptake was reduced in the disproportionately thickened septum of patients with HCM. They, however, suggested that the septal fatty acid metabolism was normal since the reduced ^{11}C-palmitate in the septum was most likely a function of decreased blood flow, and the clearance half-time of the early rapid phase and the residual fraction of ^{11}C-palmitate were similar in the septum and the lateral wall. The difference in septal fatty acid uptake between our study and theirs may be in part due to the difference between the metabolic tracers: ^{11}C-palmitate can be metabolized via beta-oxidation, while ^{123}I-BMIPP hardly can be metabolized.

Grover-McKay et al. (*6*), demonstrated moreover that ^{18}F-2-deoxyglucose uptake was lower in the septum than in the lateral wall. The decrease in septal glucose utilization accompanied by the flow-dependent decrease in β-oxidation of fatty acids may result in a decreased myocardial adenosine triphosphate concentration, which may partly explain the reduced septal uptake of ^{123}I-BMIPP (*31,33*).

Miller et al. (*10*) reported that the severely ischemic myocardium demonstrated an excess of BMIPP accumulation over perfusion measured with ^{201}Tl. They suggested that it was due to abnormal retention of BMIPP. The lesser accumulation of ^{123}I-BMIPP than ^{201}Tl observed in our

patients is likely to be neither due to flow-dependent reduction in ^{123}I-BMIPP delivery nor to abnormal retention of ^{123}I-BMIPP induced by severe ischemia. The uncoupling of ^{201}Tl and ^{123}I-BMIPP in HCM may not reflect secondary changes induced by ischemia but the intrinsic impairment of myocardial metabolism.

Limitations of the Study

Our study has several limitations. First, ^{123}I-BMIPP imaging was not performed in healthy subjects since our study was performed as a Phase 2 clinical trial. We thus could not compare the ^{123}I-BMIPP images in patients with HCM with those in normal controls. Earlier experimental studies using β-methyl fatty acid (*19,24–26*), however, showed that its myocardial distribution was almost consistent with that of regional perfusion in normal animals. Furthermore, the Phase 1 trial of myocardial imaging with ^{123}I-BMIPP in Japan revealed that the myocardial distribution of ^{123}I-BMIPP in normal volunteers was as homogeneous as that of ^{201}Tl (*34*).

Second, we could not evaluate absolute myocardial uptakes of ^{123}I-BMIPP, due mainly to conventional ECT. If they had been measured, myocardial ^{123}I-BMIPP imaging in patients with HCM might have shown not only regional heterogeneity but also a global abnormality of uptake.

Third, our patients did not form a homogeneous group but consisted of three types of HCM. They ranged in age from 21 to 75 yr. Patient 9, an elderly patient with a history of severe hypertension, might represent hypertensive HCM of the elderly (*35,36*). Further studies are needed to clarify the characteristic features of individual types of HCM (*37*).

Fourth, strict comparison between ^{201}Tl and ^{123}I-BMIPP images was impossible because they were acquired separately. Simultaneous dual-energy acquisition would provide more precise anatomical comparison. It may, however, cause errors in quantification of the uptake of each tracer (*38*).

Lastly, we should mention two technical problems. One was a partial volume effect, which is common to all imaging techniques. It causes an underestimation of regional uptakes when myocardial wall thickness is less than twice the spatial resolution of the imaging devices (*39*). However, in the comparison of RRU between ^{201}Tl and ^{123}I-BMIPP for the same region, the partial volume effect cancels out because it is the same for both tracers. The differences observed in our study were therefore unlikely to be artifacts of the partial volume effect. Another was the spatial resolution of our imaging system. The resolution (FWHM = 21 mm) was too poor to discriminate the endocardium from the epicardium. Therefore, we measured the apparent ventricular size using a region of interect generated by the peak points on each radius (*22*).

Clinical Implications

We demonstrated that myocardial ECT with ^{123}I-BMIPP may elucidate characteristic features different from ^{201}Tl imaging in patients with HCM. Our observations suggest that ECT with ^{123}I-BMIPP may detect regional abnormalities in patients with HCM earlier than ECT with ^{201}Tl. In addition, a combination of ^{201}Tl and ^{123}I-BMIPP imaging may be useful for the evaluation of various cardiomyopathies, including ischemic (*40*), hypertensive and dilated cardiomyopathies.

ACKNOWLEDGMENTS

Iodine-123-BMIPP was kindly supplied by Nihon Medi-Physics Co., Ltd., Nishinomiya, Japan. We are grateful to Ms. Yachiyo Itoh, Mr. Shinji Sakamoto, Mr. Michifumi Sawada and Ms. Tomiko Tanahashi of the Radioisotope Division for their assistance.

REFERENCES

1. Schelbert HR, Phelps ME, Shine KI. Imaging metabolism and biochemistry—a new look at the heart. *Am Heart J* 1983;105:522–526.
2. Geltman EM, Smith JL, Beecher D, Ludbrook PA, Ter-Pogossian MM, Sobel BE. Altered regional myocardial metabolism in congestive cardiomyopathy detected by positron tomography. *Am J Med* 1983;74:773–785.
3. Perloff JK, Henze E, Schelbert HR. Alterations in regional myocardial metabolism, perfusion, and wall motion in Duchenne muscular dystrophy studied by radionuclide imaging. *Circulation* 1984;69:33–42.
4. Sochor H, Schelbert HR, Schwaiger M, Henze E, Phelps ME. Studies of fatty acid metabolism with positron emission tomography in patients with cardiomyopathy. *Eur J Nucl Med* 1986;12:S66–S69.
5. Schelbert HR, Henze E, Sochor H, et al. Effects of substrate availability on myocardial C-11 palmitate kinetics by positron with ventricular dysfunction. *Am Heart J* 1986;111:1055–1064.
6. Grover-McKay M, Schwaiger M, Krivokapich J, Perloff JK, Phelps ME, Schelbert HR. Regional myocardial blood flow and metabolism at rest in mildly symptomatic patients with hypertrophic cardioimyopathy. *J Am Coll Cardiol* 1989;13:317–324.
7. Hock A, Freundlieb C, Vyska K, Losse B, Erbel R, Feinendegen LE. Myocardial imaging and metabolic studies with [17-^{123}I]iodoheptadecanoic acid in patients with idiopathic congestive cardiomyopathy. *J Nucl Med* 1983;24:22–28.
8. Rabinovitch MA, Kalff V, Allen R, et al. ω-^{123}I-hexadecanoic acid metabolic probe of cardiomyopathy. *Eur J Nucl Med* 1985;10:222–227.
9. Ugolini V, Hansen CL, Kulkarni PV, Jansen DE, Akers MS, Corbett JR. Abnormal myocardial fatty acid metabolism in dilated cardiomyopathy detected by iodine-123 phenylpentadecanoic acid and tomographic imaging. *Am J Cardiol* 1988;62:923–928.
10. Miller DD, Gill JB, Livni E, et al. Fatty acid analogue accumulation: a marker of myocyte viability in ischemic reperfused myocardium. *Circ Res* 1988;63:681–692.
11. Nishimura T, Sago M, Kihara K, et al. Fatty acid myocardial imaging using ^{123}I-β-methyl-iodophenylpentadecanoic acid (BMIPP): comparison of myocardial perfusion and fatty acid utilization in canine myocardial infarction (occlusion and reperfusion model). *Eur J Nucl Med* 1989;15:341–345.
12. Wolfe CL, Kennedy PL, Kulkarni PV, Jansen CE, Gabliani GI, Corbett JR. Iodine-123 phenylpentadecanoic acid myocardial scintigraphy in patients with left ventricular hypertrophy: alterations in left ventricular distribution and utilization. *Am Heart J* 1990;119:1338–1347.
13. Nagata S, Park Y-D, Minamikawa T, et al. Thallium perfusion and cardiac enzyme abnormalities in patients with familial hypertrophic cardiomyopathy. *Am Heart J* 1985;109:1317–1322.
14. Dunn RF, Uren RF, Sadick N, et al. Comparison of thallium-201 scanning in idiopathic dilated cardiomyopathy and severe coronary artery disease. *Circulation* 1982;66:804–810.
15. O'Gara PT, Bonow RO, Maron BJ, et al. Myocardial perfusion abnormalities in patients with hypertrophic cardiomyopathy: assessment with thallium-201 emission computed tomography. *Circulation* 1987;76:1214–1223.
16. Kurata C, Sakata K, Taguchi T, et al. SPECT imaging with Tl-201 and Ga-67 in myocardial sarcoidosis. *Clin Nucl Med* 1990;15:408–411.

17. DePuey EG, Guertler-Krawczynska E, Perkins JV, Robbins WL, Welchel JD, Clements SD. Alterations in myocardial thallium-201 distribution in patients with chronic systemic hypertension undergoing single-proton emission computed tomography. *Am J Cardiol* 1988;62:234–238.
18. Von Dohlen TW, Prisant LM, Frank MJ. Significance of positive or negative thallium-201 scintigraphy in hypertrophic cardiomyopathy. *Am J Cardiol* 1989;64:498–503.
19. Kurata C, Kobayashi A, Yamazaki N. Dual-tracer autoradiographic study with thallium-201 and radioiodinated fatty acid in cardiomyopathic hamsters. *J Nucl Med* 1989;30:80–87.
20. Sahn DJ, DeMaria A, Kisslo J, Weyman A. Recommendation regarding quantitation in M-mode echocardiography: results of a survey of echocardiographic measurements. *Circulation* 1978;58:1072–1083.
21. Yamaguchi H, Ishimura T, Nishiyama S, et al. Hypertrophic nonobstructive cardiomyopathy with giant negative T wave (apical hypertrophy): ventriculographic and echocardiogaphic features in 30 patients. *Am J Cardiol* 1979;44:401–412.
22. Takeishi Y, Tono-oka I, Ikeda K, Komatani A, Tsuiki K, Yasui S. Dilatation of the left ventricular cavity on dipyridamole thallium-201 imaging: a new marker of triple-vessel disease. *Am Heart J* 1991;121:466–475.
23. Kubota K, Som P, Oster ZH, et al. Detection of cardiomyopathy in an animal model using quantitative autoradiography. *J Nucl Med* 1988;29:1697–1703.
24. Yonekura Y, Brill AB, Som P, et al. Regional myocardial substrate uptake in hypertensive rats: a quantitative autoradiographic measurement. *Science* 1985;227:1494–1496.
25. Yamamoto K, Som P, Brill AB, et al. Dual-tracer autoradiogaphic study of β-methyl-(1-^{14}C)heptadecanoic acid and 15-p-(^{131}I)-iodophenyl-β-methylpentadecanoic acid in normotensive and hypertensive rats. *J Nucl Med* 1986;27:1178–1183.
26. Kagaya Y, Kanno Y, Takeyama D, et al. Effects of long-term pressure overload on regional myocardial glucose and free fatty acid uptake in rats: a quantitative autoradiographic study. *Circulation* 1990;81:1353–1361.
27. Goodman MM, Kirsch G, Knapp FF. Synthesis and evaluation of radioiodinated terminal p-iodophenyl-substituted α- and β-methyl-branched fatty acids. *J Med Chem* 1984;27:390–397.
28. Fujibayashi Y, Yonekura Y, Kawai K, et al. Basic studies on I-123-beta-methyl-p-iodophenylpentadecanoic acid (BMIPP) for myocardial functional diagnosis: effect of beta-oxidation inhibitor. *Jpn J Nucl Med* 1988;25:1131–1135.
29. DeGrado TR, Holden JE, Ng CK, Raffel DM, Gatley SJ. β-Methyl-15-p-iodophenylpentadecanoic acid metabolism and kinetics in the isolated rat heart. *Eur J Nucl Med* 1989;15:78–80.
30. Knapp FF, Ambrose KR, Goodman MM. New radioiodinated methyl-branched fatty acids for cardiac studies. *Eur J Nucl Med* 1986;12:S39–S44.
31. Fujibayashi Y, Yonekura Y, Takemura Y, et al. Myocardial accumulation of iodinated beta-methyl-branched fatty acid analogue, iodine-125-15-(p-iodophenyl)-3-(R,S)methylpentadecanoic acid (BMIPP), in relation to ATP concentration. *J Nucl Med* 1990;31:1818–1822.
32. Knapp FF, Ambrose KR, Dudczak R, Reske SN, Kropp J. Catabolism of 15-(p-iodophenyl)-3-R,S-methyl-pentadecanoic acid (BMIPP) by isolated rat hearts. *Eur J Nucl Med* 1989;16:367–368.
33. Ogata M. Myocardial uptake of ^{125}I-BMIPP in rats treated with adriamycin. *Jpn J Nucl Med* 1989;26:69–76.
34. Itoh H, Yamaguchi H, Ohtani M, et al. Clinical application of ^{123}I-BMIPP, a myocardial imaging agent for fatty acid metabolism. *Jpn J Nucl Med* 1990;27:1041.
35. Topol EJ, Traill TA, Fortuin NJ. Hypertensive hypertrophic cardiomyopathy of the elderly. *N Engl J Med* 1985;312:277–283.
36. Karam R, Lever HM, Healy BP. Hypertensive hypertrophic cardiomyopathy or hypertrophic cardiomyopathy with hypertension?: a study of 78 patients. *J Am Coll Cardiol* 1989;13:580–584.
37. Davies MJ. Hypertrophic cardiomyopathy: one disease or several? *Br Heart J* 1990;63:263–264.
38. Nakajima K, Taki J, Bunko H, et al. Error of uptake in dual-energy acquisition with ^{201}Tl and ^{123}I-labeled radiopharmaceuticals. *Eur J Nucl Med* 1990;16:595–599.
39. Hoffman EJ, Huang SC, Phelps ME. Quantitation in positron computed tomography. 1. Effect of object size. *J Comput Assist Tomogr* 1979;3:299–308.
40. Strauss HW, Yasuda T, Gold HK, et al. Potential role of combined fatty acid and thallium imaging in patients with myocardial ischemia and infarction. *J Nucl Med* 1987;28:632.